



# Toxic Impacts of Amorphous Silica Nanoparticles on Liver and Kidney of Male Adult Rats: an In Vivo Study

Rehab A. Azouz<sup>1</sup> · Reda M. S. Korany<sup>2</sup>

Received: 17 July 2020 / Accepted: 9 September 2020 / Published online: 22 September 2020  
© Springer Science+Business Media, LLC, part of Springer Nature 2020

## Abstract

The toxic effects of the amorphous silica nanoparticles have not been thoroughly studied. Moreover, the majority of the in vivo investigations were performed using an inhalation exposure method. The current study aimed to explore the potential toxic effects of silica nanoparticles (SiNPs) after the treatment of adult male rats with two different concentrations (500 and 1000 ppm) via drinking water for 28 days. The genotoxicity, antioxidant status, and liver and kidney functions were assessed. Besides, histopathological and immunohistochemical evaluations were performed. The results showed a significant elevation in the malondialdehyde (MDA) level concurrent with a reduction in total reduced glutathione (GSH) concentration and catalase activity in the 1000-ppm SiNP-exposed rats as well as increase in ALT and AST activity confirmed by various histopathological alterations detected in liver. Also, in the 1000-ppm SiNP-exposed animals, there was an elevation in urea and creatinine levels confirmed by histopathological alterations detected in kidneys. Immunohistochemical findings in both liver and kidneys indicated strong expression of caspase-3 in the 1000-ppm SiNP-treated rats compared with the control and 500-ppm SiNP-treated groups. Such findings indicated that the 1000-ppm SiNPs exerted severe hepato-renal toxic impacts when compared with the control and 500-ppm SiNP-exposed rats.

**Keywords** Nanosilica · Oxidative stress · Genotoxicity · Histopathology · Apoptosis

## Introduction

Nanoparticles have been extensively used in various fields, and the toxic effects on the environment and humans are attracting increasing attention. Amorphous silica nanoparticles (SiNPs) are one of the most common nanoparticles and because of their physicochemical properties; they are applied increasingly in agriculture, industrial manufacturing, construction, microelectronics, cosmetics, consumer products, and foodstuffs [1–3]. Due to their high hydrophilicity and good biocompatibility, SiNPs are developed for many biomedical and pharmaceutical applications such as drug delivery and cancer therapy, imaging probes, biosensors, and enzyme immobilization [4, 5].

Nowadays, the industrial production of SiNPs has resulted in an increased risk of human exposures at workplaces [6]. Also, SiNPs could be intentionally used for disease diagnosis and treatments [7]. As human exposure to the SiNPs is increasing, the assessment of the toxicity of these nanomaterials is urgently needed [8]. Nanosilica might lead to multiple organ damage [9]. As previously reported, SiNP exposure leads to oxidative damage and inflammatory response followed by cell membrane damage, genotoxic effect, mitochondrial dysfunction, cell cycle arrest, necrosis, and apoptosis [10, 11].

Inhalation of nanosilica produces lung inflammation, heart damage, and elevation in fibrinogen concentration and blood viscosity [12]. Nanosilica exposure also results in hydroxyl radical production [13] and hepatic injury [14, 15]. A wide range of toxic mechanisms have been reported including DNA damage and cellular nucleoplasmic protein aggregates [16], metabonomics [17], oxidative stress, and apoptosis [18, 19].

However, in vivo toxicity of SiNPs has been studied far less than in vitro toxicity [4]. Besides, there are little data about the adverse effects of SiNPs after oral administration. Thus, the present study was conducted to evaluate the toxic potential of two concentrations of SiNP in adult male rats

✉ Rehab A. Azouz  
rehab.azouz@cu.edu.eg

<sup>1</sup> Toxicology and Forensic Medicine Department, Veterinary Medicine, Cairo University, Giza, Egypt

<sup>2</sup> Pathology Department, Faculty of Veterinary Medicine, Cairo University, Giza, Egypt

through assessment of the liver and kidney function, genotoxic effect, and histopathological and immunohistochemical changes as well as appraising the antioxidant status following exposure to SiNPs.

## Materials and Methods

### Chemicals

SiNPs were purchased from Sigma-Aldrich. They were spherical and porous in shape, with a size of 20–30 nm and a purity of 99.5%. Kits for the biochemical analysis were purchased from the Biodiagnostic Company (Dokki, Giza, Egypt).

### Suspension Preparation of SiNPs

Solutions of SiNPs were prepared by sonication according to the method of Canesi et al. [20] using Sonics Vibra-Cell sonicator (Newtown, Connecticut, USA). Before the experiment, the solutions were sonicated in an ice bath for 15 min at 100 W, 50% on/off cycle.

### Animal Grouping and Experimental Design

Thirty adult male Sprague Dawley rats at 8 weeks and 180–200 g were obtained from the Faculty of Veterinary Medicine-University of Sadat City, Egypt. Rats had ad libitum access to basal ration and tap water. All rats were acclimatized for 2 weeks before the beginning of the experiment. Animal handling and treatment procedures were conducted according to the Guidelines for the Care and Use of Laboratory Animals of the National Institutes of Health (NIH) and approved by the research ethics committee of the Faculty of Veterinary Medicine, Cairo University (VetCU1022019079). For the experiments, rats were randomly distributed into three equal groups ( $n = 10/\text{group}$ ). Rats in group I (Control) received distilled water, group II received 500 ppm SiNPs in drinking water, and group III received 1000 ppm SiNPs in drinking water for 28 days. SiNP concentrations were selected according to Sadek et al. [21].

### Blood and Tissue Sampling

At the end of the study, the blood samples were collected from the retro-orbital venous plexus of control and treated rats, where it was divided into 2 parts. The first part was allowed to clot at room temperature, then centrifuged at 3000 rpm for 10 min for separation of serum which was stored at  $-20\text{ }^{\circ}\text{C}$  for biochemical analysis, while the other part was collected in heparinized tubes and immediately used for micronucleus assessment. The liver and kidney were homogenized in ice-cold 100-mM phosphate buffer (pH 7.4). The homogenates were

centrifuged at  $14,000\times g$  for 20 min, and the resulting supernatant was kept at  $-20\text{ }^{\circ}\text{C}$  for antioxidant parameters assessment. At necropsy, the liver and kidney were removed, washed with physiological saline, and weighed. Small portions of them were collected and fixed in 10% buffered neutral formalin solution for histopathological and immunohistochemical examinations.

### Genotoxicity and Cytotoxicity Biomarkers

#### 1. Micronucleus assay

Drops of whole blood were directly smeared on slides. The slides were air-dried for 24 h, fixed in methanol for 10 min, followed by 10% Giemsa staining. To detect micronuclei in erythrocytes, the slides were analyzed using a 1000-oil-immersion lens. The mean frequency of micronuclei was evaluated per 1000 cells per group of rats [22].

#### 2. Oxidative stress evaluation

The malondialdehyde was determined in homogenates by monitoring the thiobarbituric acid reactive substance (TBARS) formation using colorimetric kits as described by Ohkawa et al. [23]. GSH was determined by the colorimetric method as mentioned by Beutler et al. [24]. The CAT activity was determined according to the method of Fossati et al. [25].

### Biochemical Evaluation

The impact of SiNPs on liver function was evaluated by measuring the activities of serum alanine aminotransferase “ALT” and aspartate aminotransferase “AST” [26]. Kidney function was evaluated by measuring serum levels of BUN [27] and creatinine [28].

### Histopathological Examination and Lesion Scoring

Samples from liver and kidneys were collected from different experimental groups, fixed in 10% neutral buffered formalin and routinely processed. The paraffin-embedded blocks were sectioned at  $5\text{ }\mu\text{m}$  thickness and stained with hematoxylin and eosin [29]. Histopathological alterations in liver and kidneys were evaluated and scored as (0) indicated no changes, (1), (2), and (3) indicated mild, moderate, and severe changes, respectively, while the grading was determined by percentage as follows: ( $< 30\%$ ) showed mild changes, ( $< 30\text{--}50\%$ ) indicated moderate changes, and changes more than 50% indicated severe changes [30, 31].

## Immunohistochemistry

Formalin-fixed, paraffin-embedded 4- $\mu$ m sections were fixed into poly-L-lysine coated slides (Thermo-Scientific, Karlsruhe, Germany). After deparaffinization and rehydration, the slides were immersed in buffer Target Retrieval Solution, pH 9.0 (Dako, Glostrup, Denmark). Peroxidase Blocking Solution (Dako, Glostrup, Denmark) was used to block the activity of endogenous peroxidase. The slides were incubated with 1 mg/ml of caspase-3 antibodies at 1:50 dilution (DAKO, Glostrup, Denmark) and immunostained with DAKO Real™ Envision™ Detection System Peroxidase/DAB+, HRP Rabbit/Mouse (Dako, Glostrup, Denmark). The positive immune reactive cells showed a brown-stained cytoplasm. The color intensity and percentage area of brown color staining were estimated by color deconvolution image J software 1.52 p software (Wayne Rasband, National Institutes of Health (USA)).

## Statistical Analysis

The statistical analysis was carried out by one-way ANOVA with setting the probability level to  $p \leq 0.05$ ; post hoc analysis of group differences was performed by LSD test. The treated groups were compared both with each other and with the untreated control group. Data were expressed as mean  $\pm$  SEM.

## Results

### Micronucleus Assay

AS displayed in Fig. 1, no significant difference in the frequency of micronucleated erythrocytes was observed between the 500 ppm SiNPs and control groups. However, MN frequencies were significantly higher in the 1000-ppm SiNP-exposed group than the control and 500-ppm SiNP-treated group ( $p \leq 0.05$ ).

### Effect of SiNPs on Oxidant/Antioxidant Markers

The changes in oxidant/antioxidant markers are shown in Table 1. The levels of MDA were significantly elevated, while the activity of catalase and the level of GSH were significantly reduced in both liver and kidney of animals of the high-dose SiNP group.

### Liver and Kidney Functions

Data presented in Table 2 indicate that the high SiNP concentration caused a significant increase ( $p < 0.05$ ) in AST and ALT activities compared with control rats. Additionally, there were statistically significant increases in BUN and creatinine

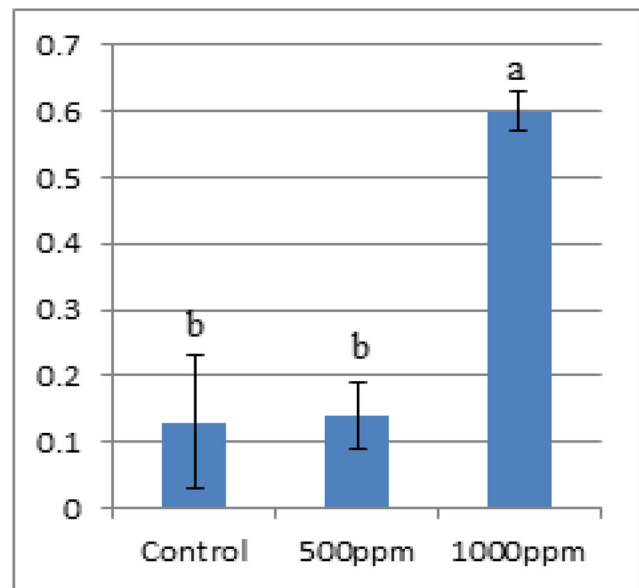


**Fig. 1** Micronuclei frequency (MN/1000 erythrocytes) of control, 500 and 1000 ppm SiNP-exposed rats. Data are expressed as mean  $\pm$  SEM,  $n = 10$ . a: Significantly different from the control group. b: Significantly different from the 1000-ppm SiNP-treated group. Using one-way ANOVA at  $p \leq 0.05$

concentrations in rats treated with 1000 ppm silica nanoparticles indicating kidney dysfunction.

### Histopathological Findings and Lesion Scoring

All the recorded lesions in the liver and kidneys were scored according to their severity as shown in Table 3. The control group showed normal histological structure of the liver (Fig. 2a and b). Concerning the group that was treated with 500 ppm SiNPs, it revealed mild vacuolar degeneration in some hepatocytes with a mild proliferation of kupffer cells (Fig. 2c and d). There was also mild congestion of hepatic

**Table 1** The oxidant/antioxidant markers in the control group and other treated groups

Parameter	Organs	Control	500 ppm	1000 ppm
MDA (nmol/g)	Liver	157 $\pm$ 4.7	157.6 $\pm$ 4.6b	188.3 $\pm$ 2.02a
	Kidney	130.6 $\pm$ 3.4	134.3 $\pm$ 2.3b	161.3 $\pm$ 2.03a
Catalase (U/g)	Liver	195.6 $\pm$ 2.8	194.6 $\pm$ 2.5b	172 $\pm$ 2.5a
	Kidney	198.3 $\pm$ 1.7	196 $\pm$ 2.6b	178 $\pm$ 1.2a
GSH (mg/g)	Liver	133.6 $\pm$ 2.7	133 $\pm$ 1.15b	85 $\pm$ 2.8a
	kidney	109.6 $\pm$ 1.45	108.3 $\pm$ 2.02b	94.3 $\pm$ 4.05a

Data are expressed as mean  $\pm$  SEM,  $n = 10$ . Rats in group I (Control) received distilled water, group II received 500 ppm SiNPs in drinking water, and group III received 1000 ppm SiNPs in drinking water for 28 days. a: Significantly different from the control group. b: Significantly different from the 1000 ppm SiNP-treated group. Using one-way ANOVA at  $p \leq 0.05$

MDA malondialdehyde, GSH reduced glutathione

**Table 2** Liver and kidney functions in all experimental groups

	AST (U/l)	ALT (U/l)	BUN (mg/dl)	Creatinine (mg/dl)
Control	86.6 ± 2.4	10.6 ± 0.8	24.6 ± 2.4	0.5 ± 0.08
SiNPs 500	88.3 ± 3.7b	11.3 ± 2.2b	26.6 ± 1.4b	0.7 ± 0.1b
SiNPs 1000	119.3 ± 2.9a	23.3 ± 3.7a	42.6 ± 4.9a	1.4 ± 0.05a

Data were expressed as mean ± SEM of 10 rats per group. Rats in group I (Control) received distilled water, group II received 500 ppm SiNPs in drinking water, and group III received 1000 ppm SiNPs in drinking water for 28 days. a: Significantly different from the control group. b: Significantly different from the 1000-ppm SiNP-treated group. Using one-way ANOVA at  $p \leq 0.05$

AST aspartate aminotransferase, ALT alanine aminotransferase, BUN blood urea nitrogen

sinusoids (Fig. 2e). Portal areas showed congestion of portal blood vessels and hyperplasia of bile duct lining epithelium (Fig. 2f). Concerning group treated with 1000 ppm SiNPs, it showed severe vacuolar degeneration of a considerable number of hepatocytes and focal coagulative necrosis of some hepatocytes. Hepatic sinusoids showed mild congestion (Fig. 3a, b, and c) with moderate proliferation of kupffer cells. Mild portal fibrosis was noticed with hyperplasia of bile duct lining epithelium.

The kidneys of the control group showed normal histological structure (Fig. 4a). Kidneys of the group treated with 500 ppm SiNPs showed congestion of glomerular tuft with vacuolation of some glomerular lining endothelium. Few renal tubules showed mild cystic dilatation (Fig. 4b and c). There was also congestion of interstitial blood vessels. Interstitial tissue revealed infiltration of mononuclear inflammatory cells (Fig. 4d). In the group that treated with 1000 ppm SiNPs, glomerular tuft revealed congestion and atrophy; also, it showed vacuolation of glomerular lining endothelium and hypercellularity. Some renal corpuscles revealed necrosis of glomerular tuft; there was also coagulative necrosis of a considerable number of renal tubular lining epithelium (Fig. 4e). Interstitial tissue revealed congestion of its blood vessels. Renal cortical interstitial tissue also showed infiltration of mononuclear

inflammatory cells (Fig. 4f), with cystic dilatation of some renal tubules.

## Immunohistochemistry

### Caspase-3 Expression

Immunostaining expression of caspase-3% area in the liver and kidneys of different groups was illustrated in Fig. 5. No caspase 3 immune-reactive cells in the liver and kidneys of control rats were observed (Fig. 6a). Sections from 500-ppm SiNP-treated group revealed weak caspase-3 expression in both liver and kidney (Fig. 6b). On the other hand, the 1000-ppm SiNP-exposed group showed strong positive immune-reactive cells in both organs (Fig. 6c).

## Discussion

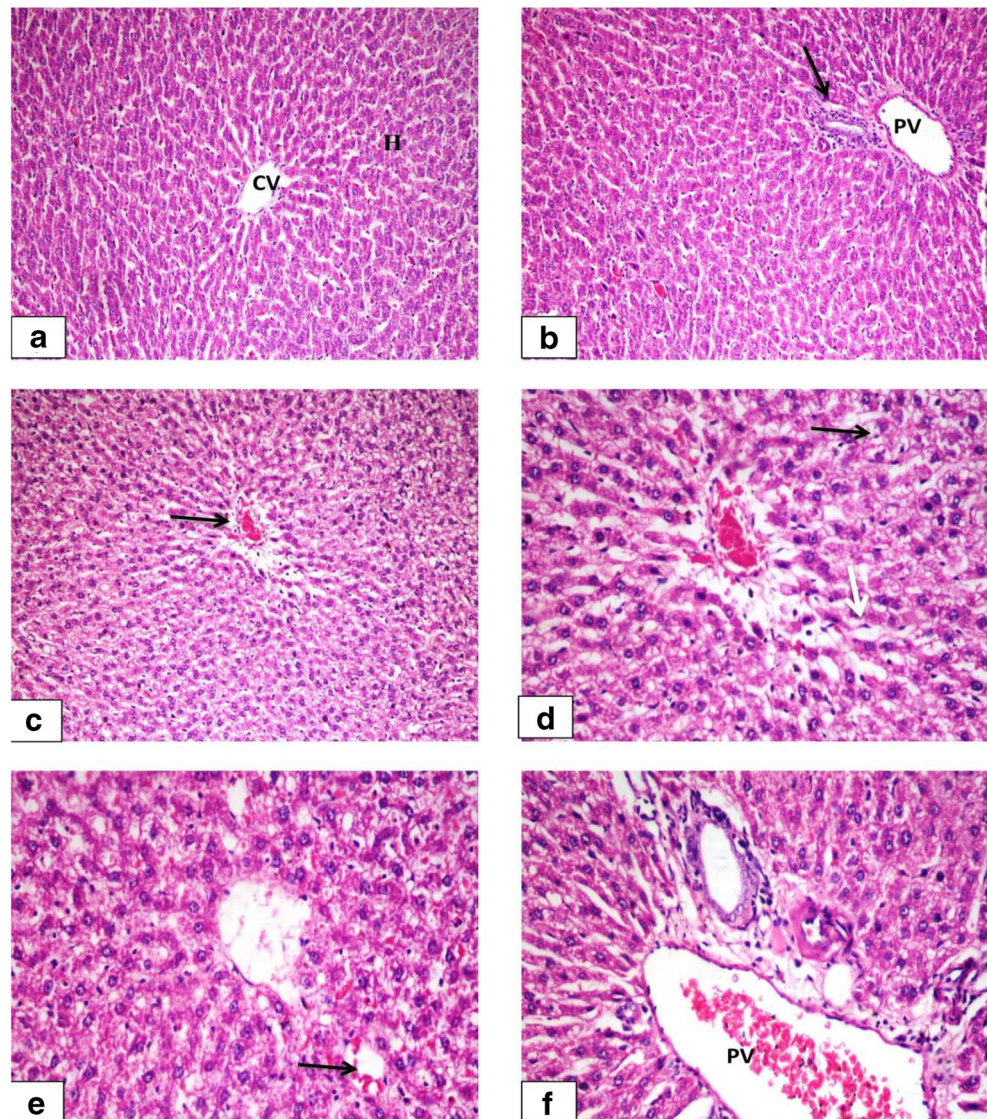
The small size of nanoparticles (NPs) was found to increase their surface area, which increases their binding to serum proteins, and their surface receptor recognition, leading to more tissue damage [32]. Because the growing production and use of SiNPs increase the risk of human exposures, an evaluation of their safety is extremely important [8, 33]. Some previous

**Table 3** Scoring of histopathological alterations in the liver and kidneys of all experimental groups

Organs	Lesions	Control	500 ppm SiNPs	1000 ppm SiNPs
Liver	- Vacuolar degeneration.	0	1	3
	- Hepatocellular necrosis.	0	1	3
	- Congestion of hepatic sinusoids.	0	1	1
	- Proliferation of kupffer cells.	0	1	2
Kidneys	- Atrophy and congestion of glomerular tuft.	0	1	3
	- Vacuolation of glomerular lining endothelium.	0	1	3
	- Hypercellularity of the glomerular tuft.	0	0	2
	- Necrosis of glomerular tuft.	0	0	2
	- Congestion of interstitial blood vessels.	0	2	3
	- Interstitial tissue infiltrated with mononuclear cells.	0	1	1
	- Necrosis of tubular lining epithelium.	0	1	3
	- Cystic dilatation of renal tubules.	0	1	2

The scoring system was designed as score 0 = absence of the lesion in all rats of the group ( $n = 5$ ), score 1 = (< 30%), score 2 = (< 30–50%), and score 3 = (> 50%)

**Fig. 2** Representative photomicrograph of rat liver. **a** Control group showing normal central vein (CV) with normal surrounding hepatocytes (H) (H&EX200). **b** Control group showing normal portal area structure (arrow) with normal portal blood vessel (PV) (H&EX200). **c** Group treated with 500 ppm SiNPs showing congestion of central vein (arrow) with mild vacuolar degeneration of surrounding hepatocytes (H&EX200). **d** Higher magnification of the previous photo showing mild vacuolar degeneration of some hepatocytes (black arrow) and proliferation of kupffer cells (white arrow) with congestion of central vein (H&EX400). **e** Group treated with 500 ppm SiNPs showing congestion of hepatic sinusoids (arrow) with mild vacuolar degeneration of hepatocytes (H&EX400). **f** Group treated with 500 ppm SiNPs showing hyperplasia of bile duct lining epithelium and congestion of portal blood vessels (PV) (H&EX400)



studies demonstrated the toxicity of silica nanoparticles on the liver and kidney of rats and mice, while other investigations reported that SiNPs have no adverse effects and can be used safely [34].

In the current study DNA damage was evaluated by the micronucleus assay. The micronucleated erythrocyte is an important marker of cellular toxicity of environmental pollutants, where the presence of micronucleus in cells is an indication of chromosomal aberrations and DNA break [35]. In our experiment, the 1000-ppm SiNP-exposed rats showed a significant elevation of micronucleus frequency as compared with that in 500 ppm SiNPs and control groups. Exposure to SiNPs resulted in DNA damage in human keratinocytes (HaCaT) [36]. Also, Exposure to nano-silica caused cell mortality and significant DNA break [37]. Nabeshi et al. [38] reported that the genotoxicity observed with nano-silica may be related to pro-inflammatory effects through ROS-mediated mechanism, modification of

chromatin structure, or elevation of DNase, a potent inducer of cytogenetic damages.

Our oxidative stress findings showed that SiNPs dose at (1000 ppm) increased the MDA content, whereas it decreased the GSH level, and CAT enzyme activity significantly. Similar to our results, oxidative stress biomarkers were significantly increased, in the serum and brain of the SiNP-exposed mice and rats [39, 40]. Further studies reported that silica NPs caused induction of oxidative damage and reactive oxygen species (ROS) generation [41, 36]. The liberation of ROS can be considered a possible mechanism for SiNP toxicity taking into consideration that silica has been shown to cause oxidative and inflammatory impacts resulting in the degradation of proteins and DNA break [42, 43]. The increase in lipid peroxidation end products could be attributed to oxidative damage of biological membranes by the generated ROS, which in turn contributes to the depletion of endogenous antioxidant enzymes and GSH amounts [44, 45]. Durairaj et al.

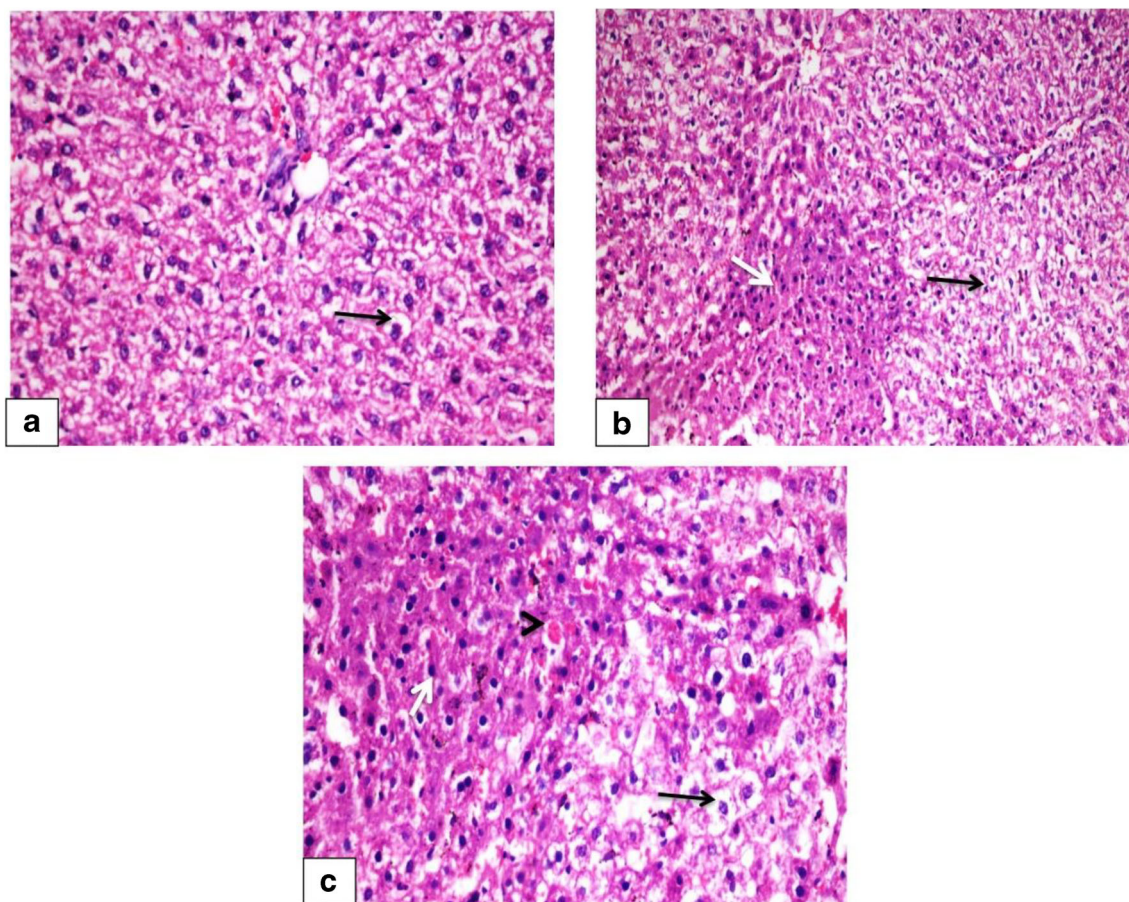


**Fig. 3** Photomicrograph of rat liver, group treated with 1000 ppm SiNPs. **a** Liver showing severe vacuolar degeneration of a considerable number of hepatocytes (arrow) (H&EX400). **b** Liver showing focal coagulative necrosis of hepatocytes (white arrow) with vacuolar degeneration of

others (black arrow) (H&EX200). **c** Higher magnification of the previous photo showing severe vacuolar degeneration of hepatocytes (black arrow), coagulative necrosis of others (white arrow), and sinusoidal dilatation (arrowhead) (H&EX400)

[46] reported that the lowering of the CAT activity may result in deleterious effects due to the accumulation of superoxide radicals and hydrogen peroxide.

Previous studies have demonstrated that NPs induced toxicological effects in different organs mainly on the lungs, liver, spleen, and kidneys [47, 48]. In the current study, the activity of serum marker enzymes of the liver (ALT and AST) were markedly elevated in rats treated with 1000 ppm SiNPs. This finding indicates hepatic damage that alters hepatocytes membrane permeability causing leakage of enzymes from the cells. In consonance with the present finding, some investigators registered an elevation in the activity of serum AST and ALT activities following SiNP administration [49, 50]. Some studies have reported that the liver is a reticuloendothelial system organ and is recognized as a major SiNP target [51, 52], as SiNPs accumulate in the liver and induce pathological changes. Previous studies have demonstrated that SiNPs inflicted severe liver damage after systemic administration [49]. Oxidative stress in the hepatic tissue of mice was notably prevalent after exposure to nano-silica, resulting in hepatic injury [53, 54].

In our study, the histopathological findings in the liver of animals treated with 500 ppm SiNPs showed mild degenerative changes in some hepatocytes with mild congestion of blood vessels, while in the group that treated with 1000 ppm SiNPs, histopathological changes included severe vacuolar degeneration of hepatocytes and focal necrosis of some. Hepatic sinusoids showed mild congestion with moderate proliferation of Kupffer cells. These results are correlated with those of oxidative stress markers and liver function tests. In one study, the ALT and AST levels were increased in SiNP-treated rats, and small amounts of inflammatory cell infiltration and hepatic cell adipose degeneration in the liver were observed [55]. The hepatic vacuolation and karyolytic and pyknotic nuclei of some hepatocytes may be due to cell injury [32].

Furthermore, our data revealed significant elevations in serum creatinine and urea in the kidney of 1000-ppm SiNP-exposed rats. The increased BUN and creatinine levels reflect reduction of glomerular filtration rate [56]. Blood biochemical parameters such as albumin, cholesterol, triglycerides, total proteins, urea, and AST activities

**Fig. 4** Representative photomicrograph of rat kidneys. **a** Control group showing normal histological structure of renal corpuscles (arrow) and renal tubules (H&EX400). **b** Group treated with 500 ppm SiNPs showing mild congestion of glomerular tuft (black arrow), note vacuolation, and necrosis of tubular lining epithelium (white arrow) (H&EX400). **c** Group treated with 500 ppm SiNPs showing vacuolation of glomerular lining endothelium (black arrow) and note coagulative necrosis of some tubular lining epithelium (white arrow) (H&EX400). **d** Group treated with 500 ppm SiNPs showing infiltration of interstitial tissue with mononuclear inflammatory cells (arrow) (H&EX200). **e** Group treated with 1000 ppm SiNPs, kidney showing severe necrosis of both glomerular lining endothelium (black arrow) and tubular lining epithelium (white arrow), and note vacuolar degeneration of glomerular lining endothelium in some corpuscles (H&EX400). **f** Kidney of group treated with 1000 ppm SiNPs showing dilatation and congestion of interstitial blood vessels (BV); interstitial tissue also showed infiltration of mononuclear inflammatory cells (arrow) (H&EX200)

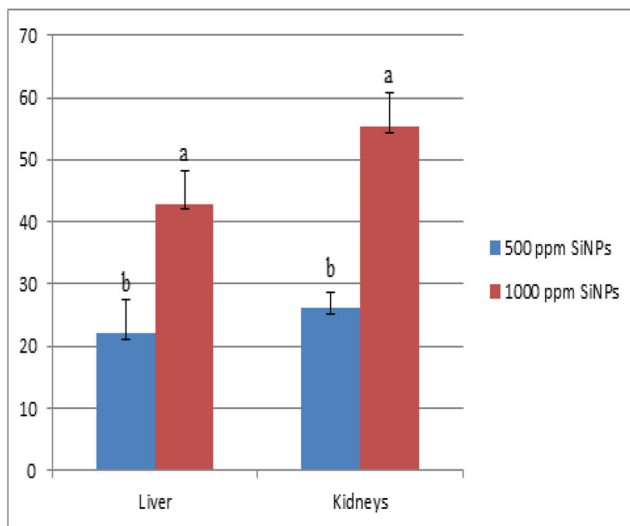
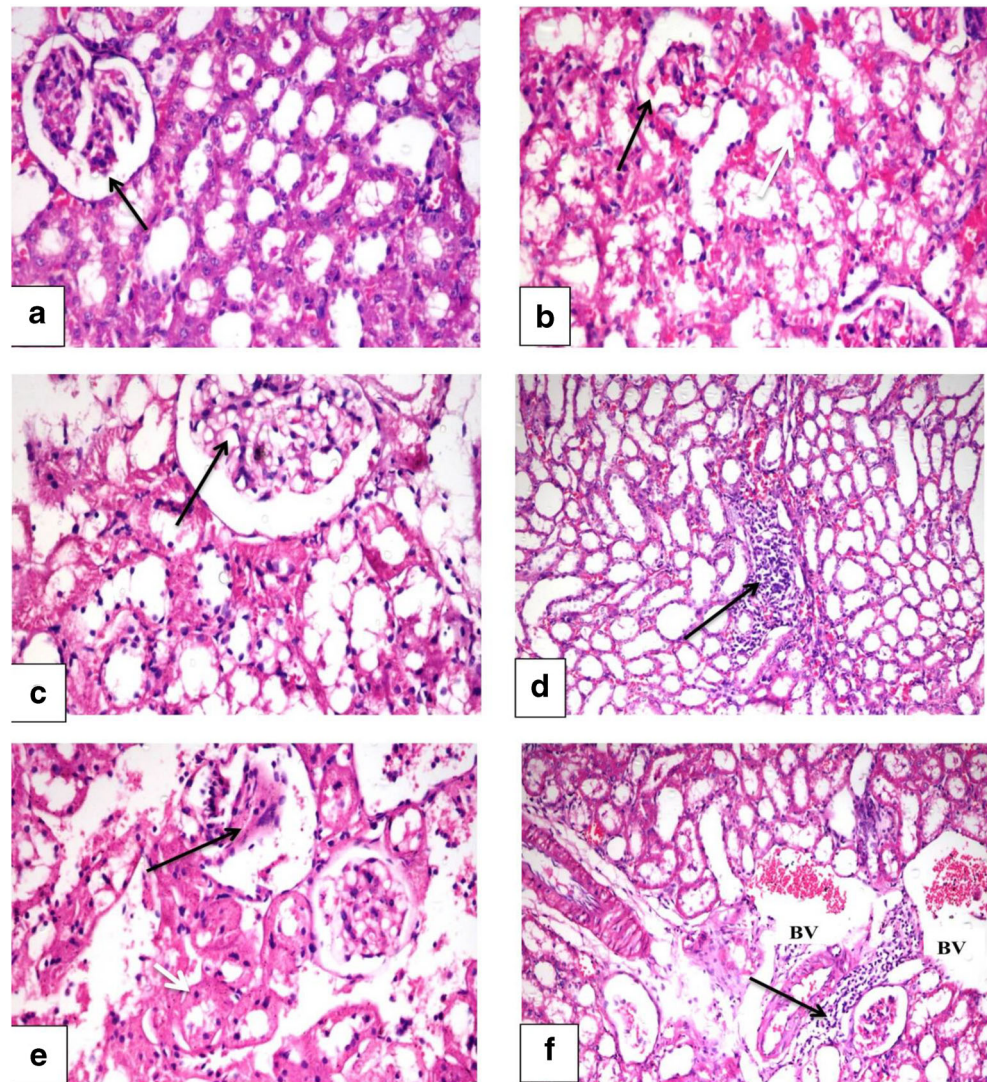
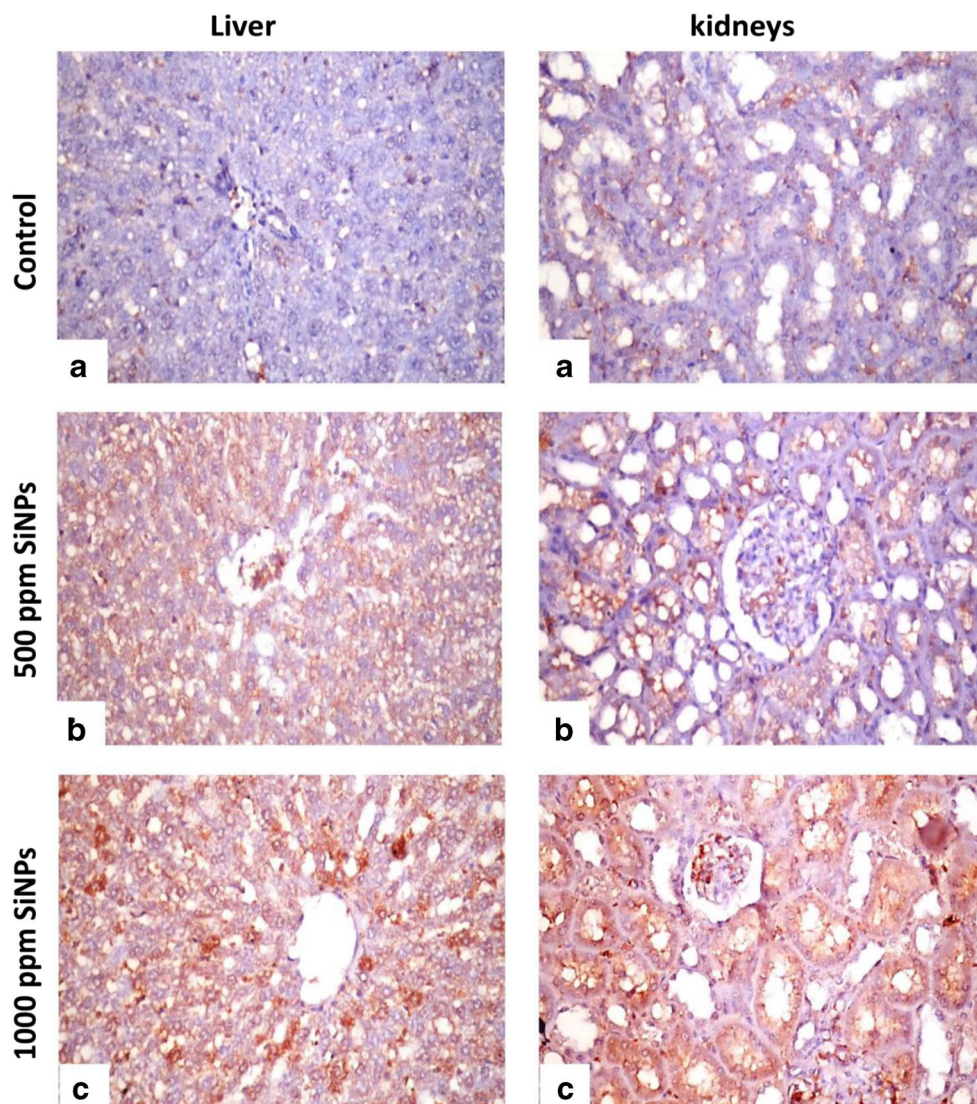


**Fig. 5** Area % of caspase-3 expression in the liver and kidneys of different experimental groups. Data are expressed as mean  $\pm$  SEM ( $n = 5$ ). Different letters in the same column were significantly different at ( $p \leq 0.05$ )

were significantly elevated in exposed mice and rats [21]. Herein, the recorded modulation in liver and kidney biochemical markers, reflecting liver and kidney injury, is in line with our histopathological and immunohistochemical findings.

Kidneys of the group treated with 500 ppm SiNPs showed mild degenerative and inflammatory reactions. In the group that treated with 1000 ppm SiNPs, glomerular tuft revealed congestion and atrophy, in addition to vacuolation of glomerular lining endothelium. Some renal corpuscles revealed necrosis of glomerular tuft. Interstitial tissue showed the infiltration of mononuclear inflammatory cells. There was coagulative necrosis of a considerable number of renal tubular lining epithelium. Hassankhani et al. [57] noticed gross tissue damage in the kidney of male mice (cell swelling and necrosis) after SiNP exposure. SiNPs were found to persist longer in liver and kidneys than any other organ [55, 58].

**Fig. 6** Immunostaining of caspase-3 in liver and kidneys. **a** Control rat showing no caspase-3 immune-reactive cells in both liver and kidneys. **b** 500-ppm SiNP-treated group showing weak positive caspase-3 expression. **c** 1000-ppm SiNP-treated group showing strong positive immune expression in both organs (Caspase-3 X400)



Immunostaining of caspase-3 protein in the liver and kidneys of the 1000-ppm SiNP-exposed group showed strong positive immune-reactive cells in both organs, and this confirmed that SiNPs induced tissue damage in both liver and kidneys by apoptosis. Oxidative stress has been reported as a toxic pathway of SiNP-induced apoptosis and inflammation in different cell types [59]. In conclusion, this study indicated that oxidative stress and apoptosis contribute to the hepato- and nephro-toxic effects of silica nanoparticles. In addition, the dose of 1000 ppm SiNPs caused marked toxicity compared with the dose of 500 ppm.

**Authors' Contributions** All authors contributed equally in the planning of the study and drafting the manuscript. All of them approve the final version of the article.

**Data Availability** All data generated or analyzed during this study are included in this published article.

## Compliance with Ethical Standards

**Conflict of Interest** The authors declare that they have no conflict of interests.

**Ethical Approval** This study was approved by the Animal Use and Care Committee at Faculty of Veterinary Medicine, Cairo University, Egypt. This study was performed after receiving ethical approval number.

**Consent for publication** All authors have reviewed the manuscript and approved its submission for publication.

## References

1. Kasai MR (2015) Nanosized particles of silica and its derivatives for applications in various branches of food and nutrition sectors. *J Nanotechnol* 2015:1–6. <https://doi.org/10.1155/2015/852394>
2. Brinch A, Hansen S, Hartmann N, Baun A (2016) EU regulation of nanobiocides: challenges in implementing the biocidal product



- regulation (BPR). *Nanomaterials* 6:33. <https://doi.org/10.3390/nano6020033>
3. Yang X, Liu X, Zhang A, Lu D, Li G, Zhang Q, Liu Q, Jiang G (2019) Distinguishing the sources of silica nanoparticles by dual isotopic fingerprinting and machine learning. *Nat Commun* 10:1620. <https://doi.org/10.1038/s41467-019-09629-5>
  4. Napierska D, Thomassen LC, Lison D, Martens JA, Hoet PH (2010) The nanosilica hazard: another variable entity. *Part Fibre Toxicol* 7:39
  5. Yu Y, Li Y, Wang W, Jin M, Du Z et al (2013) Acute toxicity of amorphous silica nanoparticles in intravenously exposed ICR mice. *PLoS ONE* 8(4):e61346. <https://doi.org/10.1371/journal.pone.0061346>
  6. Oh S, Kim B, Kim H (2014) Comparison of nanoparticle exposures between fumed and sol-gel nano-silica manufacturing facilities. *Ind Health* 52:190–198. <https://doi.org/10.2486/indhealth.2013-0117>
  7. Croissant JG, Fatieiev Y, Khashab NM (2017) Degradability and clearance of silicon, organosilica, silsesquioxane, silica mixed oxide, and mesoporous silica nanoparticles. *Adv Mater* 29(9):1–51
  8. Murugadoss S, Lison D, Godderis L, Brule SV, Mast J et al (2017) Toxicology of silica nanoparticles: an update. *Arch Toxicol* 91:2967–3010
  9. Ying N, LiZhu X, Chang B, Tong Z, Cao W et al., (2016) Nanosilica and polyacrylate/nanosilica: a comparative study of acute toxicity. *BioMed Res Int Volume Article ID 9353275*, 7 pages
  10. Aillon KL, Xie Y, el-Gendy N, Berkland CJ, Forrest ML (2009) Effects of nanomaterial physicochemical properties on in vivo toxicity. *Adv Drug Deliv Rev* 61:457–466
  11. Sun L, Li Y, Liu X, Jin M, Zhang L, du Z, Guo C, Huang P, Sun Z (2011) Cytotoxicity and mitochondrial damage caused by silica nanoparticles. *Toxicol in Vitro* 25:1619–1629. <https://doi.org/10.1016/j.tiv.2011.06.012>
  12. Chen Z, Meng H, Xing G, Yuan H, Zhao F, Liu R, Chang X, Gao X, Wang T, Jia G, Ye C, Chai Z, Zhao Y (2008) Age-related differences in pulmonary and cardiovascular responses to SiO<sub>2</sub> nanoparticle inhalation: nanotoxicity has susceptible population. *Environ Sci Technol* 42(23):8985–8992
  13. Shang Y, Zhu T, Li Y, Zhao JC (2009) Size-dependently hydroxyl radicals generation induced by SiO<sub>2</sub> ultra-fine particles: the role of surface iron. *Sci China Series B:Chem* 52(7):1033–1041
  14. Chen Y, Chen J, Dong J, Jin Y (2004) Comparing study of the effect of nanosized silicon dioxide and microsized silicon dioxide on fibrogenesis in rats. *Toxicol Ind Health* 20(1–5):21–27
  15. Van der Zande M, Vandebriel RJ, Groot MJ et al (2014) Subchronic toxicity study in rats orally exposed to nanostructured silica. *Particle Fibre Toxicol* 11(8)
  16. Chen M, Von Mikecz A (2005) Formation of nucleoplasmic protein aggregates impairs nuclear function in response to SiO<sub>2</sub> nanoparticles. *Exp Cell Res* 305(1):51–62
  17. Choi J, Zheng Q, Katz HE, Guilarte TR (2010) Silica based nanoparticle uptake and cellular response by primary microglia. *Environ Health Perspect* 118(5):589–595
  18. Lin WYW, Huang X, Zhou D, Ma Y (2006) In vitro toxicity of silica nanoparticles in human lung cancer cells. *Toxicol Appl Pharmacol* 217(3):252–259
  19. Yang XF, Liu JJ, He HW et al (2010) SiO<sub>2</sub> nanoparticles induce cytotoxicity and protein expression alteration in HaCaT cells. *Particle Fibre Toxicol* 7(1)
  20. Canesi L, Ciacci C, Vallotto D, Gallo G, Marcomini A, Pojana G (2010) In vitro effects of suspensions of selected nanoparticles (C60 fullerene, TiO<sub>2</sub>, SiO<sub>2</sub>) on *Mytilus* hemocytes. *Aquat Toxicol* 96:151–158
  21. Sadek A, Soliman M, Marzouk M (2014) Ameliorative effect of *Alloebophora caliginosa* extract on hepatotoxicity induced by silicon dioxide nanoparticles. *Toxicol Ind Health* 32(8):1358–1372
  22. Henry EH, Jenness BM, Debbie S (1997) A direct comparison of mouse and rat bone marrow and blood as target tissues in the micronucleus assay. *Mutat Res/Genet Toxicol Environ Mutagen* 391(1–2):87–89
  23. Ohkawa H, Ohishi W, Yagi K (1979) Assay for lipid peroxides in animal tissues by thiobarbituric acid reaction. *Anal Biochem* 95:351–358
  24. Beutler E, Duron O, Kelly BM (1963) Improved methods for the determination of glutathione. *J Lab Clin Med* 61:882–888
  25. Fossati P, Prencipe L, Berti G (1980) Use of 3,5-dichloro-2-hydroxybenzenesulfonic acid/4-aminophenazone chromogenic system in direct enzymic assay of uric acid in serum and urine. *Clin Chem* 26:227–237
  26. Reitman S, Frankel S (1957) Colorimetric determination of serum oxalacetic and glutamic pyruvic transaminase. *Amer J Clin Pathol* 28:56–63
  27. Fawcett JK, Scott JE (1960) A rapid and precise method for the determination of urea. *J Clin Pathol* 13:156–159
  28. Schirmeister J, Willmann H, Kiefer H (1964) Plasma creatinine as rough indicator of renal function. *Dtsch Med Wochenschr* 89:1018–1023
  29. Bancroft D, Stevens A, Turner R (2012) *Theory and practice of histological technique*, 4th edn. Churchill, Livingstone
  30. Ahmed KA, Korany RMS, El-Halawany HA, Ahmed KS (2019) *Spirulina platensis* alleviates arsenic-induced toxicity in male rats: biochemical, histopathological and immunohistochemical studies. *Adv Anim Vet Sci* 7(8):701–710
  31. Korany RMS, Ahmed KS, Halawany HA, Ahmed KA (2019) Effect of long-term arsenic exposure on female Albino rats with special reference to the protective role of *Spirulina platensis*. *Explor Anim Med Res* 9(2):125–136
  32. Fattin SM, Abd ElSalam NF, Bahaa N, Baher W (2017) Effect of silica oxide nanoparticles on liver of adult male albino rat. *Light and electron microscopic study. Egypt J Histol* 40(3):345–361
  33. Park HJ, Chung HE, Lee JA et al (2014) Quantitative determination of silica nanoparticles in biological matrices and their pharmacokinetics and toxicokinetics in rats. *Sci Adv Mater* 6(6):1605–1610. <https://doi.org/10.1166/sam.2014.1817>
  34. Comelekoglu U, Balli E, Yalin S, Eroglu P, Bayrak G, Yaman S, Sogut F (2019) Effects of different sizes silica nanoparticle on the liver, kidney and brain in rats: Biochemical and histopathological evaluation. *J Res Pharm* 23(3):344–353
  35. Azouz RA, AbuBakr HO, Khatib MS, Abou-Zeid SM. (2020) Buprofenin toxication implicates health hazards in Nile tilapia (*Oreochromis niloticus*). *Aquat Res* 00:1–12
  36. Gong C, Tao G, Yang L et al (2012) The role of reactive oxygen species in silicon dioxide nanoparticle-induced cytotoxicity and DNA damage in HaCaT cells. *Mol Biol Rep* 39:4915–4925. <https://doi.org/10.1007/s11033-011-1287-z>
  37. Gerloff K, Albrecht C, Boots AW, Förster I, Schins RPF (2009) Cytotoxicity and oxidative DNA damage by nanoparticles in human intestinal Caco-2 cells. *Nanotoxicology*. 3:355–364
  38. Nabeshi HT, Yoshikawa K, Matsuyama Y, Nakazato S, Tochigi S et al (2011) Amorphous nanosilica induce endocytosis-dependent ROS generation and DNA damage in human keratinocytes. *Part Fibre Toxicol* 8:1
  39. Du Z, Zhao D, Jing L et al (2013) Cardiovascular toxicity of different sizes amorphous silica nanoparticles in rats after intratracheal instillation. *Cardiovasc Toxicol* 13:194–207. <https://doi.org/10.1007/s12012-013-9198-y>
  40. Parveen A, Rizvi SHM, Sushma et al (2015) Intranasal exposure to silica nanoparticles induce alterations in pro-inflammatory environment of rat brain: involvement of oxidative stress. *Toxicol Ind Health* 33:119–132. <https://doi.org/10.1177/0748233715602985>
  41. Kim YJ, Yu M, Park HO, Yang SI (2010) Comparative study of cytotoxicity, oxidative stress and genotoxicity induced by silica

- nanomaterials in human neuronal cell line. *Mol Cell Toxicol* 6:336–343
42. Passagne I, Morille M, Rousset M, Pujalte I, L'Azou B (2012) Implication of oxidative stress in size-dependent toxicity of silica nanoparticles in kidney cells. *Toxicology* 299:112–124
  43. Duan J, Yu Y, Li Y, Yu Y, Li Y, Zhou X, Huang P, Sun Z (2013) Toxic effect of silica nanoparticles on endothelial cells through DNA damage response via Chk1-dependent G2/M checkpoint. *PLoS ONE* 8:e62087
  44. Kong XH, Wang GZ, Li SJ (2007) Antioxidation and ATPase activity in the gill of mud crab *Scylla serrata* under cold stress. *Chin J Oceanol Limnol* 25:221–226
  45. Akhtar MJ, Ahamed M, Kumar S, Siddiqui H, Patil G, Ashqin M, Ahmad I (2010) Nanotoxicity of pure silica mediated through oxidant generation rather than glutathione depletion in human lung epithelial cells. *Toxicology* 276:95–102
  46. Durairaj A, Vaiyapuri TS, Kanti MU et al (2008) Protective activity and antioxidant potential of *Lippia nodiflora* extract in paracetamol induced hepatotoxicity in rats. *Iran J Pharmacol Ther* 7:83–89
  47. Chen Z, Meng H, Xing G, Chen C, Zhao Y, Jia G, Wang T, Yuan H, Ye C, Zhao F, Chai Z, Zhu C, Fang X, Ma B, Wan L (2006) Acute toxicological effects of copper nanoparticles in vivo. *Toxicol Lett* 163:109–120
  48. Wang J, Zhou G, Chen C et al (2007) Acute toxicity and biodistribution of different-sized titanium dioxide particles in mice after oral administration. *Toxicol Lett* 168:176–185
  49. Liu T, Li L, Teng X et al (2011) Single and repeated dose toxicity of mesoporous hollow silica nanoparticles in intravenously exposed mice. *Biomaterials* 32:1657–1668
  50. Fu C, Liu T, Tang F, Chen D, Li LL, Liu HY, Li XM (2012) Acute toxicity and oxidative damage induced by silica nanorattle in vivo. *Chin Sci Bull* 57:2525–2532
  51. Kumar R, Roy I, Ohulchanskyy TY, Vathy LA, Bergey EJ, Sajjad M, Prasad PN (2010) In vivo bio distribution and clearance studies using multimodal organically modified silica nanoparticles. *ACS Nano* 4:699–708
  52. Lee S, Kim M, Lee D, Kwon TK, Khang D, Yun H, Kim S (2013) The comparative immunotoxicity of mesoporous silica nanoparticles and colloidal silica nanoparticles in mice. *Int J Nanomedicine* 8:147–158
  53. So SJ, Jang IS, Han CS (2008) Effect of micro/nano silica particle feeding for mice. *J Nanosci Nanotechnol* 8(10):5367–5371
  54. Ye Y, Liu J, Chen M, Sun L, Lan M (2010) In vitro toxicity of silica nanoparticles in myocardial cells. *Environ Toxicol Pharmacol* 29:131–137
  55. Lai LC, Qian X, Ming CW, Jin F, Na Na S, Peng ZX, Ning LY, Hui Y et al (2018) Subchronic oral toxicity of silica nanoparticles and silica microparticles in rats. *Biomed Environ Sci* 31(3):197–207
  56. Naziroglu M, Karaoglu A, Aksoy AO (2004) Selenium and higher dose vitamin E administration protects cisplatin induced oxidative damage to renal, liver, lens tissues in rats. *Toxicology* 195:221–230
  57. Hassankhani R, Esmaeillou M, Tehrani AA et al (2014) In vivo toxicity of orally administrated silicon dioxide nanoparticles in healthy adult mice. *Environ Sci Pollut Res*. <https://doi.org/10.1007/s11356-014-3413-7>
  58. Lee J, Kim M, Paek H, Kim Y, Kim M, Lee J, Jeong J, Choi S (2014) Tissue distribution and excretion kinetics of orally administered silica nanoparticles in rats. *Int J Nanomedicine* 9:251–260
  59. Park EJ, Park K (2009) Oxidative stress and proinflammatory responses induced by silica nanoparticles in vivo and in vitro. *Toxicol Lett* 184:18–25

**Publisher's Note** Springer Nature remains neutral with regard to jurisdictional claims in published maps and institutional affiliations.